Journal of ELECTRONIC MATERIALS, Vol. 41, No. 3, 2012
DOI: 10.1007/s11664-011-1829-0

Stress Relaxation in Sn-Based Films: Effects of Pb Alloying, Grain Size, and Microstructure

NITIN JADHAV,[1,2] JACOB WASSERMAN,[1] FEI PEI,[1] and ERIC CHASON[1]

1.—School of Engineering, Brown University, Providence, RI 02912, USA. 2.—e-mail: nitin_jadhav@brown.edu

Stress is believed to provide the driving force for growth of Sn whiskers, so stress relaxation in the Sn layer plays a key role in their formation. To understand and enhance stress relaxation in Sn-based films, the effects of Pb alloying and microstructure on their mechanical properties have been studied by observing the relaxation of thermal expansion-induced strain. The relaxation rate is found to increase with film thickness and grain size in pure Sn films, and it depends on the microstructure in Pb-alloyed Sn films. Measurements of multilayered structures (Sn on Pb-Sn and Pb-Sn on Sn) show that changing the surface layer alone is not sufficient to enhance the relaxation, indicating that the Pb enhances relaxation in the bulk of the film and not by surface modification. Implications of our results for whisker mitigation strategies are discussed.

Key words: Sn whisker, packaging, tin, whisker, thermal expansion-induced strain, Pb-free solder, thermal stress, surface modification

INTRODUCTION

Sn-based coatings are commonly used in the electronics industry as protective layers over conductors on printed wiring boards and connectors.[1] In addition, their low melting temperature makes them ideal candidates for use as solder material. Although alloys containing Pb have been used for years,[2] increasing concerns about environmental effects and corresponding legislation have pushed the industry towards Pb-free manufacturing.[3]

One of the biggest concerns with the removal of Pb from Sn films is the formation of Sn whiskers, i.e., thin filaments that grow spontaneously out of the film's surface. Typically a few microns in diameter, whiskers can be a few microns to a few millimeters in length,[4–6] enough to come into contact with nearby conductive surfaces and cause failures due to short circuits and arcing.[7] Although first discovered 50 years ago,[8] they have not been a reliability concern until recently because alloying with Pb effectively eliminates whisker formation.[9]

(Received May 13, 2011; accepted November 18, 2011; published online December 9, 2011)

Sn whiskers are broadly believed to form in response to stress in the Sn layer,[10–12] which has been attributed to the formation of an intermetallic compound (IMC) Cu_6Sn_5 in the Sn layer near the Sn–Cu interface.[11] Reduction of stress in the Sn layer can therefore reduce the driving force for whisker formation and be used as a means for whisker mitigation. Zhang and Schwagers[13] suggested that Pb reduces whiskering by forming more uniform IMC layers that create less compressive stress in the Sn. Alternatively, Boettinger et al. proposed enhanced creep relaxation in Pb-Sn alloys due to the presence of horizontal grain boundaries in the more equiaxed microstructure relative to the columnar structure of pure Sn.[14] In a previous study[12] comparing Sn and Pb-Sn films, we showed that addition of Pb decreases the compressive stress in the film even though the rate of IMC formation is not altered significantly. Yu et al.[15] have also shown that changing the microstructure of the top and/or bottom of the layer can modify the whisker growth. Other research works suggest that stress gradient may also play a role in whiskering.[16–19]

The work described above has focused primarily on correlating whisker density with the Sn properties, so its interpretation is complicated by the

simultaneous evolution of the IMC and the stress. To better understand the evolution of the stress apart from the IMC formation, in the current study we have directly measured stress relaxation behavior in films deposited on Si substrates without any Cu layer present. To produce stress without the formation of IMC, the samples were subjected to cycles of heating and cooling. As the sample was heated, the film developed compressive stress due to the mismatch in the coefficient of thermal expansion (CTE) between the film and the substrate, and the corresponding film stress was monitored using a wafer curvature technique. The sample was then held at a constant elevated temperature so that the stress relaxation kinetics due to creep could be measured. The creep behavior was measured for films with different microstructure, thickness, and alloy composition; creep relaxation rates were observed to be faster for films with larger Sn thickness and grain size and for thick Pb-containing alloys. We also observed that surface modification of a Sn film by the addition of a Pb-Sn overlayer does not change its creep behavior, indicating that the effect of Pb in enhancing stress relaxation occurs in the film's bulk.

EXPERIMENTAL PROCEDURES

Stress measurements were performed on various electroplated Sn-based thin-film samples. The samples were prepared on silicon substrates (200 μm thick, rectangular in shape, 25.4 mm $\times$ 12.5 mm) made from (001)-oriented single-crystal Si with both sides polished and a 100-nm-thick surface oxide (SiO_2) layer. A seed layer of 0.5-μm Sn was deposited by physical vapor deposition (PVD) to provide a conducting surface for the subsequent electroplated Sn layer. PVD was performed in a Temescal electron-beam evaporator under vacuum of 4.0×10^{-4} Pa. A 15-nm layer of titanium was deposited prior to the Sn layer to enhance the adhesion between the Sn and the Si substrate. The substrates were cleaned before deposition using a standardized leaning procedure [5 min each in acetone, methanol, and deionized (DI) water with ultrasonic agitation, followed by drying with compressed nitrogen gas].

The final film layers (alloy Sn and pure Sn) were electroplated over the seed layer using a commercial Sn (pure tin) and SnPb (tin with approximately 10% lead) plating solution (Solderon SC, produced by Rohm & Haas). A three-electrode electrodepositing cell controlled by a potentiostat with a saturated calomel (SCE) reference electrode was used for the film deposition. In addition to the single uniform layers, samples with multiple layers were also prepared to study the effect of surface modification on stress relaxation behavior. During the multiplating process the cell was taken out from one plating solution cell and was placed in DI water before inserting the cell into the other bath. This was done to avoid contamination from the previous bath. The plating solution, being an acidic bath, removed any oxide layer that may have formed on the seed layer as well as on the electroplated layer during the multideposition. After electrodeposition, the samples were then rinsed twice with DI water for 30 s and dried by dry nitrogen. The thicknesses of the samples were measured using a Dektak profilometer and were also verified by measuring the weight gain due to plating. After deposition, the samples were stored under ambient conditions for about 24 h while the stress was monitored to relax the stress due to plating so that the residual stress in the samples was minimal.

The film stress was measured using a wafer curvature technique known as multibeam optical stress sensor (MOSS),[20] in which the curvature of the sample is measured optically. As shown in Fig. 1, the sample is placed on a heating stage with the uncoated side of the Si substrate facing the optical system. A glass slide under the Sn-coated sample surface prevents the film from reacting with the metal stage. The temperature of the sample is measured using a thermocouple attached to a similar silicon wafer placed 0.5 cm away from the actual sample. The optical system (laser plus etalon) produces an array of parallel laser beams that are reflected off the highly reflective substrate surface into a charge-coupled device (CCD) camera. By measuring the spacing between the beams, changes in the curvature ($1/R$) of the sample can be measured, which can then be related to the average film stress by Stoney's equation

$$\frac{1}{R} = \frac{6\sigma h_f}{M_s h_s^2},$$

where h_f and h_s are the film and substrate thickness, respectively, M_s is the biaxial modulus of the substrate, and $\langle\sigma\rangle$ is the stress in the film averaged over the thickness of the layer. This setup allows us to measure curvature and thus stress in real time while the film experiences heating/cooling cycles and while being held at elevated temperature.

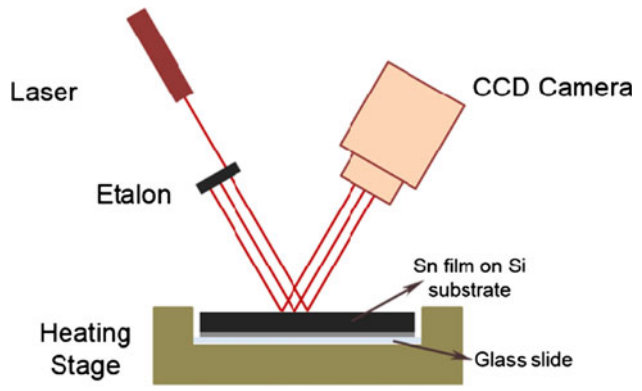

Fig. 1. Schematic of a heating stage and multibeam optical stress sensor (MOSS) system. The back side of the Si substrate is facing upward to reflect the laser beams.

Figure 2 shows three heating cycles that were performed on each sample. Each heating cycle consisted of four stages. In the first stage, the samples were heated at constant rate of 0.5°C/min from room temperature (23°C) to 33°C (ΔT = 10°C), 43°C (ΔT = 20°C), or 63°C (ΔT = 40°C). During the second stage, the samples were held at the desired temperature (33°C, 43°C, or 63°C) for 6 h. After this isothermal relaxation, the samples were then air-cooled to room temperature during the third stage. In the fourth and final stage, the samples were monitored at room temperature for 6 h to 8 h.

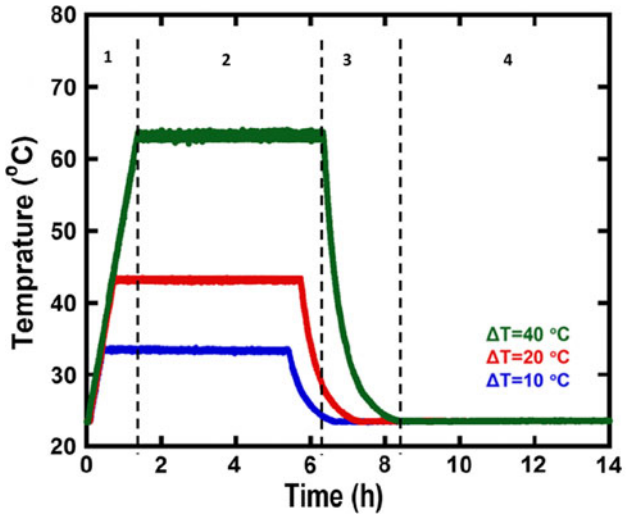

Fig. 2. Temperature profile of the heating cycles that samples underwent. The vertical dashed lines demarcate the four different stages of the ΔT = 40°C heating cycle, corresponding to: stage 1, heating at 0.5°C/min from room temperature (24°C); stage 2, holding the sample for 300 min; stage 3, air-cooling; stage 4, monitoring at room temperature for 6 h to 8 h.

Each of these three cycles was performed on the different samples while the curvature was monitored simultaneously. As the samples were heated, they built up compressive stress due to the thermal mismatch between the Si substrate ($\sim 3.2 \times 10^{-6}$/K) and the Sn-based layer ($\sim 22 \times 10^{-6}$/K). Measurements of stress in the 0.5-μm Sn seed layer alone were performed so that its contribution to the curvature could be subtracted from the total when calculating the average stress in the sample. The effects of changes in the microstructure of the seed layer during plating are discussed in later sections. The contribution of the 15-nm Ti layer (vapor deposited on Si for better adhesion) was neglected because of its very small thickness.

Figure 3a shows the stress profile in one such sample as it underwent the three cycles. To observe the microstructure of the films, apart from scanning electron microscopy (SEM), a focused ion beam (FIB) was used to obtain a view of their cross-section.

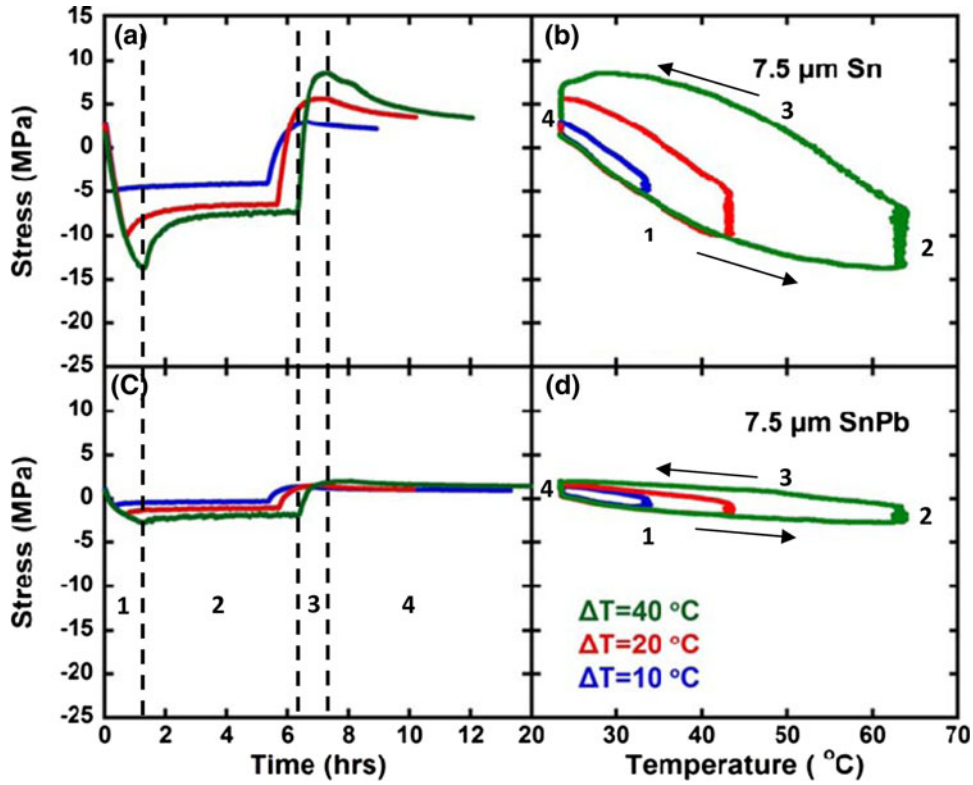

Fig. 3. Stress versus time and temperature during thermal cycling for (a, b) 7.5-μm Sn layer and (c, d) 7.5-μm Pb-Sn alloy layer. The numbers (1, 2, 3, 4) in (a–d) indicate the four different stages of the heating cycle (stage 1, heating; stage 2, holding; stage 3, air-cooling; stage 4, room-temperature monitoring) and the arrows in (b, d) indicate the direction of the thermal cycles.

Table I. Details of samples fabricated and measured

Sample Number	Description	Detail
1	Thick Sn film	7.5-μm pure Sn film
2	Thick Pb-Sn alloy film	7.5-μm Sn alloyed with 10% Pb film
3	Thin Sn film	1-μm pure Sn film
4	Thin Pb-Sn alloy film	1-μm Sn alloyed with 10% Pb film
5	Thick Sn with Pb-Sn alloy surface layer	7.5-μm pure Sn film and 1-μm Sn alloyed with 10% Pb film on top
6	Thick Pb-Sn alloy with Sn surface layer	7.5-μm Sn alloyed with 10% Pb film and 1-μm pure Sn film on top

To study the effects of microstructure and Pb alloying on stress relaxation, a number of sample structures were fabricated and measured (Table I). The thickness refers to the electroplated layer and does not include the 0.5-μm seed layer that was deposited by PVD. The multilayer structures (5 and 6) were produced to separate the effect of stress relaxation at the surface of the film from stress relaxation in the bulk of the layer. To obtain a film structure with surface properties of Pb-Sn alloy and bulk properties of Sn, a relatively thin Pb-Sn alloy film was plated on top of a thick Sn layer. Similarly, to get Sn-like surface properties on a Pb-Sn alloy layer, a thin Sn layer was electroplated on top of the Pb-Sn alloy.

RESULTS AND DISCUSSION

Difference in Response of Pb-Alloy and Pure Sn Films to Thermally Induced Stress

Figure 3a shows the stress evolution as a function of time in the 8-μm pure Sn film as it underwent the heating cycles shown in Fig. 2. The vertical dashed lines in the two figures indicate the transition between different heating regimes for the highest-temperature cycle. As the temperature is increased initially, the stress is compressive due to the larger thermal expansion coefficient of Sn. At first the stress grows at the same rate for each curve, indicating that the film is in the elastic regime. At later times, the curves start to diverge from linearity due to the onset of stress relaxation. After the sample reaches the final temperature (34°C, 44°C, and 64°C, respectively, for the three heating cycles), additional stress relaxation can be observed as the temperature is held constant for 300 min. As the sample is air-cooled after being held at the high temperature, it develops tensile stress, again due to the larger thermal expansion of the Sn relative to the substrate. The final dashed line corresponds to the continued stress relaxation after the sample reaches room temperature.

The change of stress with temperature (ΔT) derived from the temperature versus time curve is shown in Fig. 3b. For correspondence with the heating cycles, the stress versus temperature cycle shown should be read in a counterclockwise direction as shown by arrows; i.e., the sample is heated from room temperature to a higher temperature, held at this elevated temperature, and then cooled again to room temperature. For small ΔT, the stress of the film increases linearly, corresponding to the elastic regime. At larger ΔT, a deviation from linearity is seen due to the onset of stress relaxation. As the curve reaches higher (lower) temperatures while heating (cooling), the slope of the curve decreases, indicating that the sample has a greater amount of relaxation as the magnitude of the thermally induced stress increases. The vertical lines in the stress are due to relaxation while being held at constant temperature after heating (right) or cooling (left). This relaxation produces a hysteresis-like behavior of the film stress over the course of the heating and cooling cycle.

For the Pb-Sn alloy sample, the stress–temperature evolution is shown in Fig. 3c, d as it underwent the same series of thermal cycles as the pure Sn sample. The sample consists of a 7.5-μm-thick alloy with 10% Pb concentration electroplated over the 0.5-μm vapor-deposited Sn seed layer. The initial slope of stress versus time is essentially the same for the 7.5-μm Sn and 7.5-μm Pb-Sn alloy samples, which indicates that the Pb addition does not change the thermal expansion coefficient or modulus of Sn drastically. However, the addition of Pb does appear to change the stress relaxation properties of the layer. As the alloyed sample is heated (Fig. 3c), the stress does not go above 3 MPa to 4 MPa, a factor of 4 to 5 times less than that observed in the pure Sn (Fig. 3a, b) for the same heating cycle. Similarly, in the graph of stress versus temperature (Fig. 3d), the magnitude of stress developed during the heating/cooling cycle is clearly less than for the pure Sn sample.

Although these experiments clearly show an enhancement of stress relaxation in Sn due to Pb alloying, the mechanism by which Pb modifies the mechanical properties cannot be determined from this single set of experiments. Therefore, we have performed other measurements to understand the nature of the relaxation process as described below.

Surface Versus Bulk Effects: How Does Pb Enhance Stress Relaxation in Sn-Alloy Films

One important question is whether the Pb alloying enhances stress relaxation by modifying the surface of the layer or whether it changes the relaxation mechanisms in the bulk of the film. It is well understood, for instance, that the surface oxide plays an important role in suppressing stress relaxation in the Sn layer by preventing diffusion of Sn atoms to the surface. We have previously shown

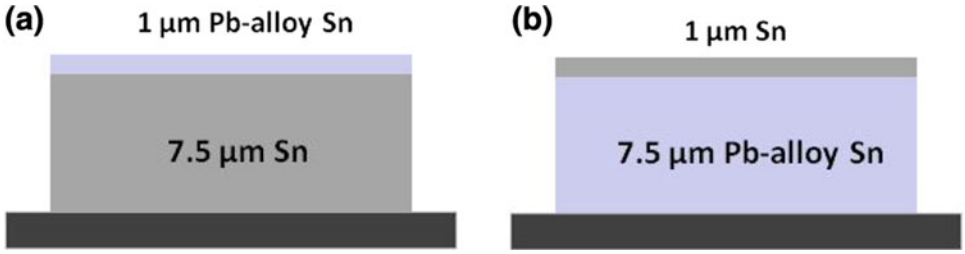

Fig. 4. Schematic showing multilayer Sn samples: (a) 1-μm Pb-Sn alloy coating on top of 7.5-μm Sn film, and (b) 1-μm Sn coating on top of 7.5-μm Pb-Sn alloy film.

that removal of the oxide in pure Sn layers can lead to rapid stress relaxation in the layer.[12] Thus it may be possible that Pb enhances stress relaxation by altering the surface oxide. However, Boettinger et al.[14] have observed that the addition of Pb modifies the microstructure of Pb-Sn alloy layers, so that the layers have a more equiaxed grain structure than the columnar microstructure found in pure Sn. They propose that the addition of numerous horizontal grain boundaries creates sinks for the dislocations and mobile point defects, which allows for the strain to be accommodated without the generation of stress. A similar mechanism was also proposed by Smetana,[21] in which whisker formation in pure Sn was described as a result of diffusion of Sn atoms to oblique grain boundaries under stress. The high concentration of horizontal grain boundaries in Pb-Sn was proposed to relax the entire Sn surface rather than an individual grain.

To differentiate between these possible mechanisms, we performed stress measurements on a set of samples grown with a multilayered structure. In the first case, a 1-μm layer of Pb-Sn alloy was grown on top of a thicker (7.5 μm) pure Sn film, so that the bulk of the layer was pure Sn while the surface consisted of a Pb-Sn alloy (shown schematically in Fig. 4a). In the second case, a 1-μm layer of pure Sn was grown on top of a 7.5-μm Pb-Sn alloy layer (Fig. 4b) so that the bulk of the film would have the Pb-Sn microstructure while the surface consisted of pure Sn. Plating of the thin surface layer over the thicker underlayer did not change its microstructure. The 7.5-μm pure Sn with a 1-μm Pb-alloyed layer on top still had a columnar structure similar to the single layer of 7.5-μm Sn, and the 7.5-μm Pb-Sn alloy with a 1-μm pure Sn layer on top had an equiaxial structure similar to just 7.5-μm Pb-Sn alloy. FIB images and further details of the microstructure are discussed below.

Figure 5 shows the mechanical response of these layered samples during the heating cycles described previously. As the Sn layer with the Pb-alloy surface is thermally cycled (Fig. 5a, b), it builds up a stress profile virtually identical to the 7.5-μm pure Sn sample (Fig. 3a, b). Similarly, when the Pb-Sn layer with the pure Sn surface is cycled (Fig. 5c, d), it builds up very little stress, analogous to the behavior of the Pb-Sn alloy film without any surface modification. This indicates that changing the surface properties of the layer does not modify the stress relaxation behavior significantly, suggesting that the alloying with Pb enhances stress relaxation through modification of the bulk properties of the film.

Effect of Film Thickness/Grain Size on Stress Relaxation in Pure Sn Films

It has been observed in many studies of Sn layers on Cu that the thickness of the Sn layer affects the system's propensity to whisker;[5,22,23] i.e., thicker layers typically have fewer whiskers than thin layers. Recently we have shown that the stress induced by IMC growth in thick layers of Sn over Cu saturates at a lower steady-state value than for thinner layers,[24] reinforcing the link between compressive stress and whisker formation. To study this more explicitly, we have measured the mechanical properties of Sn-based layers with different thickness during thermal cycling with no Cu present so that the mechanical behavior could be studied without any interference from other factors such as IMC formation.

Figure 6 shows the stress response during a heating cycle of a 1-μm pure Sn film for comparison with the 7.5-μm Sn film (Fig. 3a, b). For small values of ΔT both the thick (7.5 μm) and thin (1 μm) Sn films have the same slope, again corresponding to the elastic regime. At larger ΔT, however, we find that for the thinner film the slope of the stress versus ΔT curve is nearly constant over the entire temperature range, indicating that the amount of plastic deformation during heating is much smaller than for the thicker film. Similarly, even after the sample is held at elevated temperature for 6 h, the thinner film has relaxed less than the thick film. We observe the same trend during cooling; i.e., the thin film stays in the elastic regime while the stress in the thick film relaxes. This enhanced relaxation behavior with thickness is consistent with our studies of Sn on Cu in which the thicker films developed less steady-state stress due to IMC formation. Figure 7 shows cross-sections of the films observed by a focused ion beam system. The grains in both thick (7.5 μm) and thin (1 μm) Sn film are columnar in shape but of different diameter, which appears to increase with an increase in thickness.

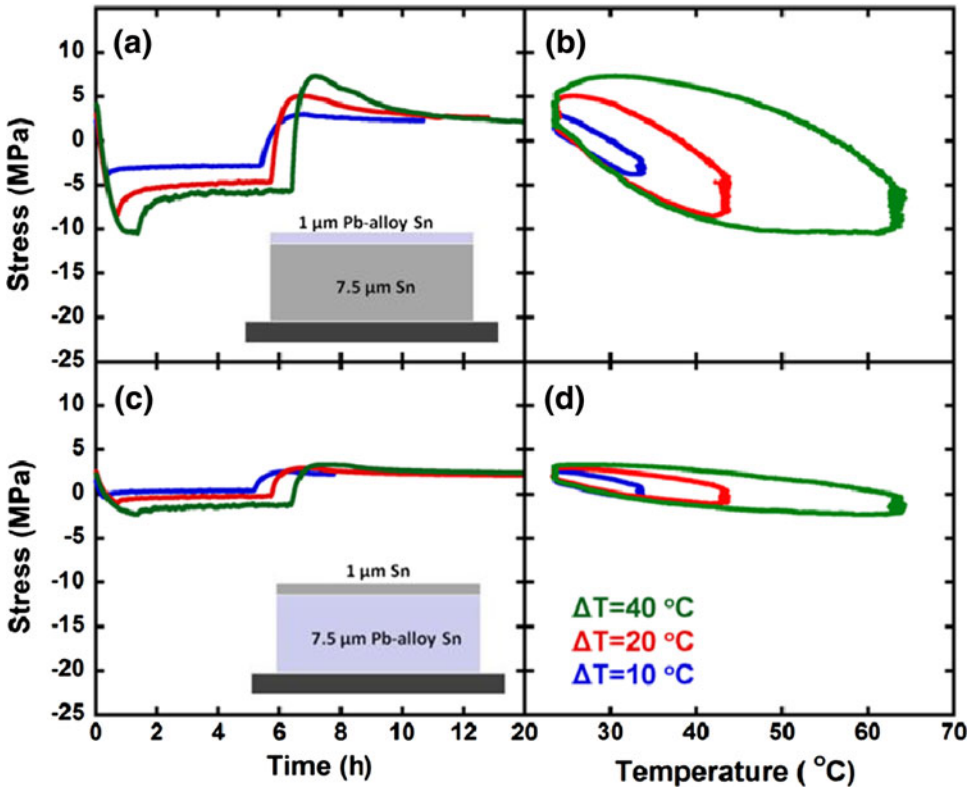

Fig. 5. Stress versus time and temperature during thermal cycling for (a, b) 7.5-μm Sn layer with 1-μm Pb-Sn alloy layer on top and (c, d) 7.5-μm Pb-Sn alloy layer with 1-μm Sn layer on top.

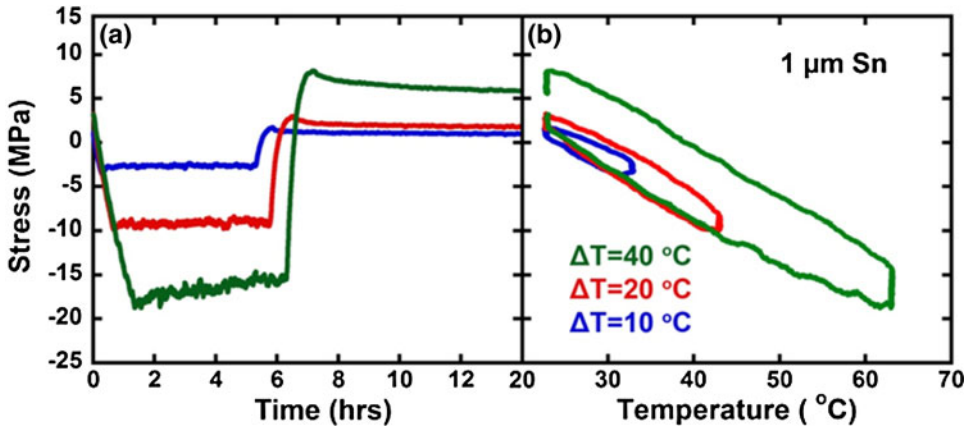

Fig. 6. Stress versus (a) time and (b) temperature during thermal cycling for 1-μm Sn layer.

Tsuji[25] has shown in his work that grain size in electroplated Sn increases proportionally to the Sn film thickness (Grain size $\propto \sqrt{\text{Thickness}}$), which we also observe in the cross-section in Fig. 7a, b. Thus the thickness dependence of the stress relaxation in thicker films may equivalently be attributed to the larger grain size as well as the film thickness. Observations of higher resistance to stress relaxation in finer-grained materials are found in many other materials.[26,27] These findings are also in agreement with various grain-size-dependent mechanisms that impede dislocation-mediated relaxation, e.g., barriers to crossing grain boundaries and strain hardening by higher density of dislocations in smaller grains.

Effect of Film Thickness/Grain Structure on Stress Relaxation in Pb-Sn Alloy Films

To determine the corresponding effect of thickness on Pb-Sn alloy layers, measurements were performed on a 1-μm Pb-Sn film (Fig. 8) for comparison with the 7.5-μm Pb-Sn film (Fig. 3c, d). We observe that the thin Pb-Sn alloy film has much less

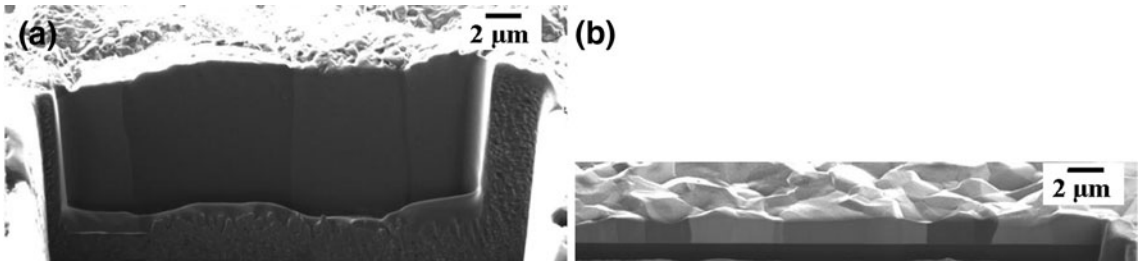

Fig. 7. Cross-section of (a) 7.5-μm Sn film, and (b) 1-μm Sn film.

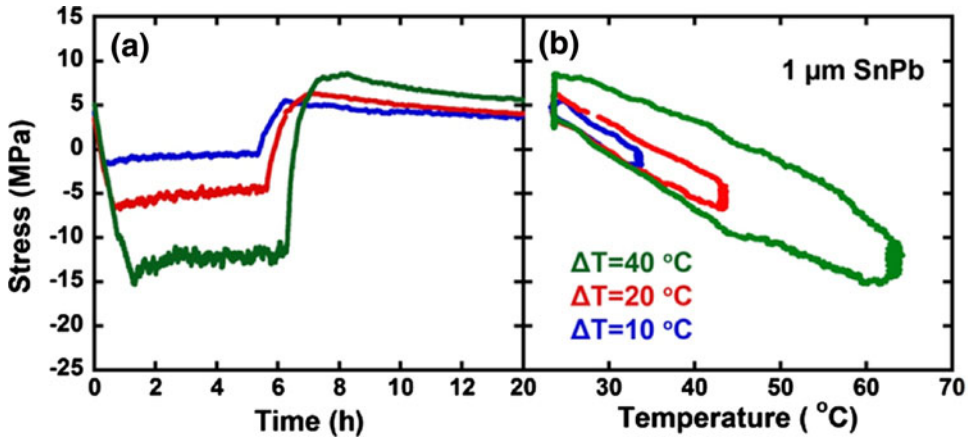

Fig. 8. Stress versus (a) time and (b) temperature during thermal cycling for 1-μm Pb-Sn alloy layer.

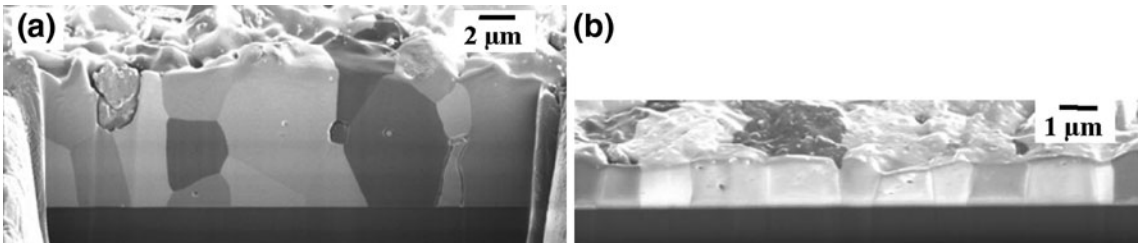

Fig. 9. Cross-sections of (a) 7.5-μm Pb-Sn alloy film, and (b) 1-μm Pb-Sn alloy film.

relaxation than the thick alloy sample. In fact, the mechanical behavior of the 1-μm Pb-alloy Sn film is similar to the behavior observed in the 1-μm pure Sn film. This is in marked contrast to the results for the 7.5-μm thick films in which the alloy layer had much greater relaxation than the pure Sn.

These measurements indicate that alloying with Pb enhances relaxation of thermally induced stress for the thicker films but not for the thinner films. To understand the origin of this, cross-sections of the thick (Fig. 9a) and thin (Fig. 9b) Pb-Sn alloy layers were measured using FIB. It is evident that the two sample thicknesses have very different microstructures. In the case of the thick samples, the grains were found to be more equiaxial, whereas the thin films had columnar grains that spanned the entire thickness of the film. This strongly supports the suggestions[14] that stress relaxation is enhanced by the horizontal grain boundaries which are present in the thick alloy films but not the thin films. It also further supports our conclusion that the surface is not responsible for the enhanced relaxation, since both the thick and thin films have the same surface composition.

The similar stress relaxation behavior for thin Pb-Sn and pure Sn at first appears to be in contradiction with our previous results for thin Sn-based layers deposited over Cu.[12] In these studies, Pb-Sn layers with approximately the same thickness (1.45 μm) showed much greater relaxation of the stress due to IMC formation than pure Sn samples of the same thickness. To understand this, we measured the microstructure of thin Pb-Sn alloy (Fig. 10a) and pure Sn (Fig. 10b) layers grown over Cu. The cross-section of the Pb-Sn alloy layer shows that it has equiaxial grains, whereas the pure Sn film on Cu has a columnar microstructure. There-

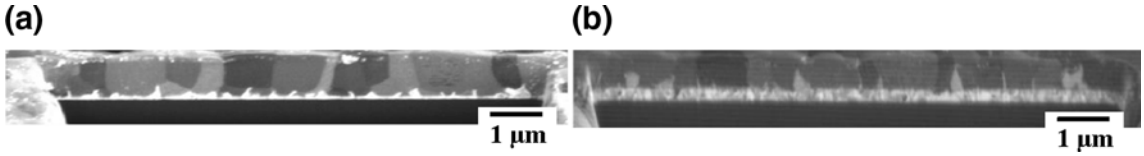

Fig. 10. Cross-sections of (a) 1-μm Pb-Sn alloy film and (b) 1-μm Sn film electroplated on a 0.6-μm vapor-deposited Cu layer.

fore, the enhanced stress relaxation behavior seems to be determined primarily by the equiaxial grain structure and presence of horizontal grain boundaries and not simply the presence of Pb in the alloy.

CONCLUSIONS

The effects of Pb alloying, layer thickness, and surface termination on the mechanical properties of Sn-based layers were studied by monitoring the evolution of thermal mismatch-induced stress. We find that, for thick (7.5 μm) layers, the addition of Pb alloying significantly increases the stress relaxation relative to pure Sn layers. In the case of the Pb-Sn alloys, the relaxation enhancement corresponds to the presence of an equiaxial microstructure with horizontal grain boundaries that can serve as sites for stress relaxation. In comparison, the pure Sn has a columnar microstructure with nearly vertical grain boundaries.

For thinner (1 μm) layers, we find much less stress relaxation for both Pb-Sn and pure Sn layers. The microstructure for both compositions is columnar, with a smaller grain size that scales with the film thickness. For the pure Sn samples, the reduction in stress relaxation appears to be due to the smaller thickness and grain size. For the alloy samples, the absence of horizontal grain boundaries appears to play a bigger role, since alloy samples of similar thickness grown on Cu that have an equiaxed grain structure display much greater stress relaxation behavior. To further determine whether horizontal grain boundaries alone are sufficient to increase stress relaxation, future measurements of other plating conditions that result in equiaxial grain structures are planned. To determine the effect of surface termination on stress relaxation behavior, we studied multilayers in which the bulk of the film was pure Sn (or Pb-Sn) with a thin surface overlayer of Pb-Sn (or pure Sn). The insensitivity of the relaxation behavior to the surface confirmed that the changes in the stress relaxation behavior must be occurring in the bulk of the film.

Finally we note that effects which lead to enhancement in the stress relaxation behavior in these experiments are also correlated with a decrease in the formation of Sn whiskers in layers grown over Cu. This supports the view that enhancing stress relaxation can serve to mitigate whisker formation.

ACKNOWLEDGEMENTS

The authors gratefully acknowledge help from Jae wook Shin and Gordon Barr and the support from the NSF under Contract DMR0856229, the NSF-sponsored MRSEC (Contract DMR0079964), and the EMC Corporation.

REFERENCES

1. S.B. Lyon, *Shreir's Corrosion*, ed. J.A.R. Tony (Oxford: Elsevier, 2010), p. 2068.
2. G.T. Galyon, *IEEE Trans. Electron. Packag. Manuf.* 28, 94 (2005).
3. S. Herat, *CLEAN-Soil Air Water* 36, 145 (2008).
4. B. Hampshire and L. Hymes, *Circuits Assembly* (2000), p. 50.
5. B. D. Dunn, *European Space Agency (ESA) STR-223* (1987).
6. N. Jadhav, E. Buchovecky, E. Chason, and A. Bower, *JOM* 62, 30 (2010).
7. NASA.
8. K.G. Compton, A. Mendizza, and S.M. Arnold, *Corrosion* 7, 327 (1951).
9. S.M. Arnold (Presented at the IEEE Electronic Components Technology Conference, unpublished, 1959).
10. B.Z. Lee and D.N. Lee, *Acta Mater.* 46, 3701 (1998).
11. K.N. Tu, *Phys. Rev. B* 49, 2030 (1994).
12. E. Chason, N. Jadhav, W.L. Chan, L. Reinbold, and K.S. Kumar, *Appl. Phys. Lett.* 92, 171901 (2008).
13. W. Zhang and F. Schwager, *J. Electrochem. Soc.* 153, C337 (2006).
14. W.J. Boettinger, C.E. Johnson, L.A. Bendersky, K.W. Moon, M.E. Williams, and G.R. Stafford, *Acta Mater.* 53, 5033 (2005).
15. C.-F. Yu, C.-M. Chan, and K.-C. Hsieh, *Microelectron. Reliab.* 50, 1146 (2010).
16. E. Chason, N. Jadhav, and F. Pei, *JOM* 63, 62 (2011).
17. J. Liang, Z.-H. Xu, and X. Li, *J. Mater. Sci.: Mater. Electron.* 18, 599 (2007).
18. Y. Sun, E.N. Hoffman, P.-S. Lam, and X. Li, *Scripta Mater.* 65, 388 (2011).
19. M. Sobiech, M. Wohlschlogel, U. Welzel, E.J. Mittemeijer, W. Hugel, A. Seekamp, W. Liu, and G.E. Ice, *Appl. Phys. Lett.* 94, 221901 (2009).
20. E. Chason and J.A. Floro, *Measurements of Stress Evolution During Thin Film Deposition* (1996).
21. J. Smetana, *IEEE Trans. Electron. Packag. Manuf.* 30, 11 (2007).
22. M. Dittes, P. Obemdorff, and L. Petit (Presented at the Electronic Components and Technology Conference, Proceedings. 53rd, unpublished, 2003).
23. C. Xu, Y. Zhang, C. Fan, J. Abys, L. Hopkins, and F. Stevie, *CircuiTree* 94–105 (2002).
24. N. Jadhav, E.J. Buchovecky, L. Reinbold, S. Kumar, A.F. Bower, and E. Chason, *IEEE Trans. Electron. Packag. Manuf.* 33, 183 (2010).
25. K. Tsuji, (Presented at the IPC/JEDEC 4th International Conference on Lead-Free Electronic Components and Assemblies, Frankfurt, Germany, unpublished, 2003).
26. Y. Choi and S. Suresh, *Acta Mater.* 50, 1881 (2002).
27. R.-M. Keller, S.P. Baker, and E. Arzt, *J. Mater. Res.* 13, 1307 (1998).